www.sciencemag.org/content/345/6203/1515/suppl/DC1

Supplementary Materials for

H3K27me and PRC2 transmit a memory of repression across generations and during development

Laura J. Gaydos, Wenchao Wang, Susan Strome*

*Corresponding author. E-mail: sstrome@ucsc.edu

Published 19 September 2014, *Science* **345**, 1515 (2014)
DOI: 10.1126/science.1255023

This PDF file includes

Materials and Methods
Figs. S1 to S7
References

Materials and Methods

Strains and culture

C. elegans were maintained on NGM (Nematode Growth Medium) agar plates using *Escherichia coli* OP50 as a food source at 15°C. Experiments were carried out at 20°C or 24°C.

The following balancers were used:
mnC1[dpy-10(e128) unc-52(e444)] II
hT2-GFP*[bli-4(e937) let(q782) qIs48] (I;III)*
DnT1-GFP*[unc(n754) let qIs51] (IV;V)*

The following strains were used:
N2 variety Bristol
SS0104 *glp-4(bn2) I*
SS1178 *glp-4(bn2) I; ccIs4811[lmn-1*::GFP + *dpy-20(+)] X*
SS0818 *mes-3(bn35) I/hT2*-GFP *(I;III)*
SS1167 *mes-3(bn35) I/hT2*-GFP *(I;III); fem-2(b245ts) III/hT2*-GFP *(I;III)*
SS1099 *mes-3(bn35) I/hT2*-GFP *(I;III); him-8(e1489) IV*
SS1133 *mes-3(bn35) I/hT2*-GFP *(I;III); met-2(n4256) set-25(n5021) III/hT2*-GFP *(I;III); him-8(e1489) IV*
SS1171 *mes-3(bn35) I/hT2*-GFP *(I;III); ccIs4811[lmn-1*::GFP + *dpy-20(+)] X*
SS1169 *mes-3(bn35) I/hT2*-GFP *(I;III); otIs181[dat-1*::mCherry + *ttx-3*::mCherry*] III/hT2*-GFP *(I;III); ccIs4811[lmn-1*::GFP + *dpy-20(+)] X*
SS1172 *mes-3(bn35) I/hT2*-GFP *(I;III); him-8(e1489) IV; ccIs4811[lmn-1*::GFP + *dpy-20(+)] X*
SS1170 *mes-3(bn35) I/hT2*-GFP *(I;III); otIs181[dat-1*::mCherry + *ttx-3*::mCherry*] III/hT2*-GFP *(I;III); him-8(e1489) IV; ccIs4811[lmn-1*::GFP + *dpy-20(+)] X*
SS0186 *mes-2(bn11)unc-4(e120)/mnC1 II*
SS1026 *unc-4(e120) II; him-8(e1489) IV*
SS1027 *mes-2(bn11) unc-4(e120)/mnC1 II; him-8(e1489) IV*
DH0245 *fem-2(b245ts) III*
unc-119(ed3) III
SS1148 *met-2(n4256) set-25(n5021) III/hT2*-GFP *(I;III)*
CB1489 *him-8(e1489) IV*
SP646 *mnT12 (IV;X)*
SS0784 *mes-6(bn38) him-8 IV/DnT1-GFP (IV;V)*
SS0782 *mes-6(bn38) IV/DnT1*-GFP *(IV;V); dpy-11(e224) V/DnT1*-GFP *(IV;V)*
AV311 *dpy-18(e364) unc-3(e151) meT7 (III;X;IV)*

Fertility assays

To test XO males for fertility, single L4-stage XO males were put on a plate with at least 6 L4 *unc-119* hermaphrodites and allowed to mate at 20°C for 4 days. Males were scored as fertile if the plate contained at least 4 non-Unc progeny (cross progeny).

Staining germline nuclei

L4 XO males were separated from hermaphrodites and incubated overnight at 20°C to allow accumulation of sperm. The next day, to remove bacteria, the males were allowed to crawl on blank agar plates for a few minutes. Males were picked into 1µl drops of water on a gelatin chrom alum-coated slide. The slide was waved over an alcohol burner flame until dry, and worms were mounted in 4',6-diamidino-2-phenylindole (DAPI) at a final concentration of 0.05µg/ml in Gelutol mounting medium. Germline nuclei were counted, and images were taken on a Zeiss Axioskop using a QImaging Retiga 2000R camera and ImageJ AquireQCam plug-in software.

Immunocytochemistry

Worms were fixed using methanol/acetone (*33*). L1 larvae were obtained by hatching embryos in the absence of food in M9 buffer and fixed after feeding for ~5 hours. L3 and L4 larvae were obtained by hatching L1s in the absence of food, then transferring L1s to a plate with food for ~24 hours (L3) or ~36 hours (L4). Embryos and larvae were fixed whole. Adults were dissected to isolate germ lines, embryos, and sperm. Dissection of germ lines and embryos was done in Egg Buffer (25mM HEPES pH 7.4, 118mM NaCl, 48mM KCl, 2mM $CaCl_2$, 2mM $MgCl_2$) with 1mM levamisole. Dissection of male germ lines containing sperm was done in Sperm Salts (50mM HEPES pH7.5, 1mM $MgSO_4$, 25mM KCl, 45mM NaCl, 5mM $CaCl_2$) with 1mM levamisole. Germ lines with sperm were separated from worm carcasses and squashed by overlaying a coverslip and wicking away excess buffer. Primary antibodies and dilutions used for immunostaining were: 1:30,000 mouse anti-H3K27me3 (Kimura mAb 1E7), 1:30,000 mouse anti-H3K27me3 (Active Motif 39535), 1:10,000 rabbit anti-H3K27me3 (Upstate 07-449), 1:30,000 mouse anti-H3K9me2 (Kimura mAb 6D11), 1:10,000 rabbit anti-H3K4me2 (Millipore 07030), 1:750 mouse anti-GFP (Roche 11814460001), 1:30,000 rabbit anti-PGL-1 (*34*). Mouse monoclonal antibodies against H3K27me3 (1E7) (*35*) and H3K9me2 (6D11) (*36*) were gifts from Hiroshi Kimura (Osaka University). Secondary antibodies conjugated to Alexa Fluor 488 or 594 (Molecular Probes) were used at 1:300 with 0.05µg/ml 4',6-diamidino-2-phenylindole (DAPI) for 2 hours at room temperature. Images were acquired with a Volocity spinning disk confocal system (Perkin Elmer/Improvision, Norwalk, CT, USA) fitted on a Nikon Eclipse TE2000-E inverted microscope. Mouse anti-H3K27me3 from H. Kimura was previously shown to be specific for that modification (*35*) and was used in all figures. Results obtained with that antibody are shown in this paper and were confirmed with anti-H3K27me3 antibodies from Active Motif and Upstate.

Quantitation of immunostaining

Wild-type and *mes-3/+* M-P+ embryos were fixed and stained with mouse anti-H3K27me3 antibody (Kimura mAb 1E7), secondary antibody, and DAPI. Stacks of optical sections were collected with the spinning disk microscope described above, and 3-D voxel intensities were analyzed using Volocity software (Release 5.1.0; http://www.improvision.com). Nuclei were identified and their boundaries were estimated in 3-D using the DAPI channel and the "Standard Deviation Intensity" function of Volocity. Within each interphase nucleus, the H3K27me3 voxel intensity sum was measured and reduced by a cytoplasmic background value (intensity sum measured in

cytoplasm for a region of similar geometry). With the staining and imaging parameters used, interphase nuclei generally did not show any oversaturation of H3K27me3 voxels; nuclei with oversaturated voxels were not included in the analysis. An average intensity sum per nucleus was then calculated for each embryo, and values were placed in sets defined by developmental stages (2-cell, 4-cell, ~8-cell, ~16-cell). Cell cycles in those stages are sufficiently synchronous to ensure that all interphase nuclei in an embryo had been through either 0, 1, 2, or 3 cell divisions, respectively, relative to the 2-cell stage. Within each stage/division category, an average nuclear H3K27me3 staining intensity sum was calculated ($n \geq 15$ embryos/stage/genotype) and normalized to the intensity sum for the 2-cell stage within that genotype.

Analysis of *lmn-1*::GFP expression in germ lines

XO males with the *lmn-1::*GFP transgene were dissected as adults, and their germ lines were fixed and stained for GFP as described for immunocytochemistry. Images were acquired on a compound microscope as described for staining germline nuclei.

Generation of M-P+ and M+P- embryos and worms

To generate M-P+ embryos, *mes-3* M+Z-; *fem-2* feminized hermaphrodites were mated with wild-type males or *mnT12 (IV;X)*/+ males, or *met-2 set-25* hermaphrodites were mated with wild-type males containing MitoTracker red-labeled sperm (*37*) and only embryos showing traces of MitoTracker red were analyzed. *mes-3* M+Z- animals inherited a maternal load of gene product but did not produce gene product from the zygotic genome and consequently lacked HMT in the parental . To generate M+P- embryos and larvae, *fem-2* feminized hermaphrodites were mated with *mes-3* M+Z- or *met-2 set-25* males. To generate M+P- embryos with fused M+ chromosomes, *dpy-18 unc-3 meT7 (III;X;IV)* hermaphrodites were mated with *mes-3* M+Z- males. Only cross progeny (showing mosaic H3K27me3) were analyzed.

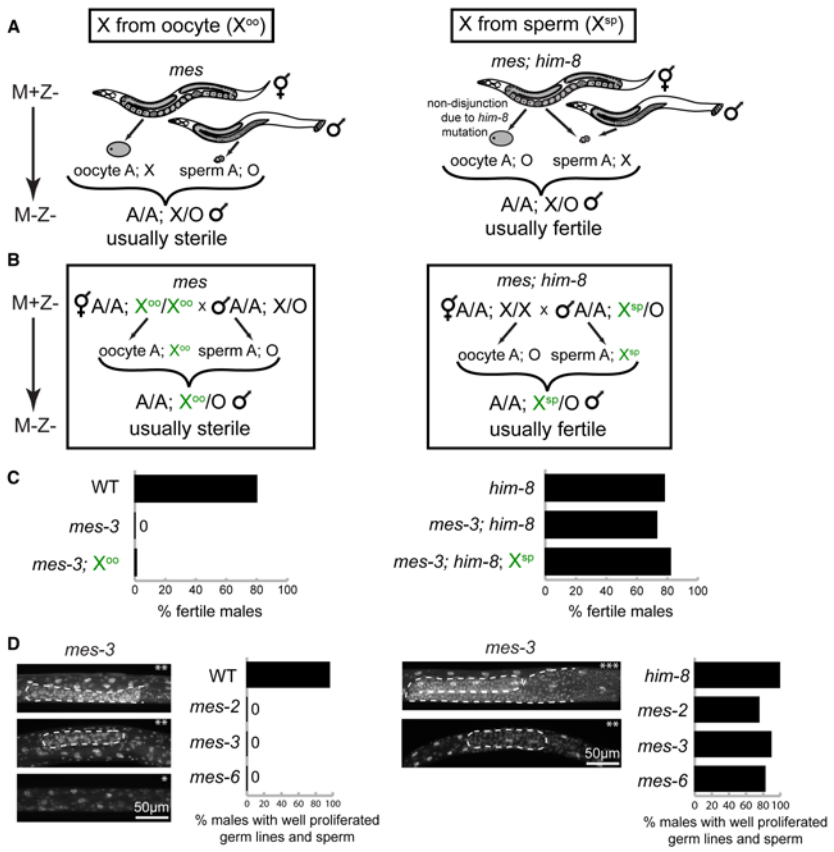

Fig. S1

Germline health and fertility of XO *mes* mutant males depend on the gamete source of the X chromosome.

A) Diagrams of crosses used to generate XO *mes* males that inherited their X chromosome from the oocyte (X^{oo}) or the sperm (X^{sp}). To generate XO (X^{oo}) *mes* males, XX hermaphrodites were mated to XO males. Male offspring resulted from the union of an X-bearing oocyte from the hermaphrodite and a nullo-X sperm from the male. XO (X^{sp}) *mes* males were generated using *him-8* XX mothers, which undergo non-disjunction of their X chromosomes predominantly during oogenesis (*38*) and produce male offspring from the union of a nullo-X oocyte and an X-bearing sperm. M is maternal supply of *mes*(+) gene product, Z is zygotic expression of the *mes*(+) gene. **B)** Diagrams of crosses used to unambiguously identify the gamete source of the X in *mes-3* males. One or the other parent contributed to progeny an X chromosome that expressed an X-linked GFP-tagged nuclear lamin transgene, *lmn-1*::GFP (shown as a green X). **C)** Fertility of control (wild-type (WT) and *him-8*) and *mes-3* males generated by the different methods described in A and B. Fertility was tested by mating single males with *unc-119* hermaphrodites and scoring for the production of non-Unc outcross progeny. Even *mes-3* XO (X^{sp}) sons from fertile *mes-3* XO (X^{sp}) fathers were fertile (69% fertile, n=48). **D)** Analysis of germ cell proliferation and presence of sperm in XO (X^{oo}) and (X^{sp}) *mes-2*, *mes-3*, and *mes-6* mutant males. Images are DAPI (DNA) staining (germ lines outlined by white dashed lines) of *mes-3*, showing well proliferated germ lines with sperm (***), under-proliferated germ lines (**), and no germ cells (*). Histograms are

percent XO *mes* mutants with well proliferated germ lines with sperm, as determined by DNA staining. *mes-3* males with X^{oo} were produced by mating *mes* hermaphrodites with *mes* males. *mes-2* males with X^{oo} and *mes-6* males with X^{oo} were produced by mating *mes* hermaphrodites with wild-type males.

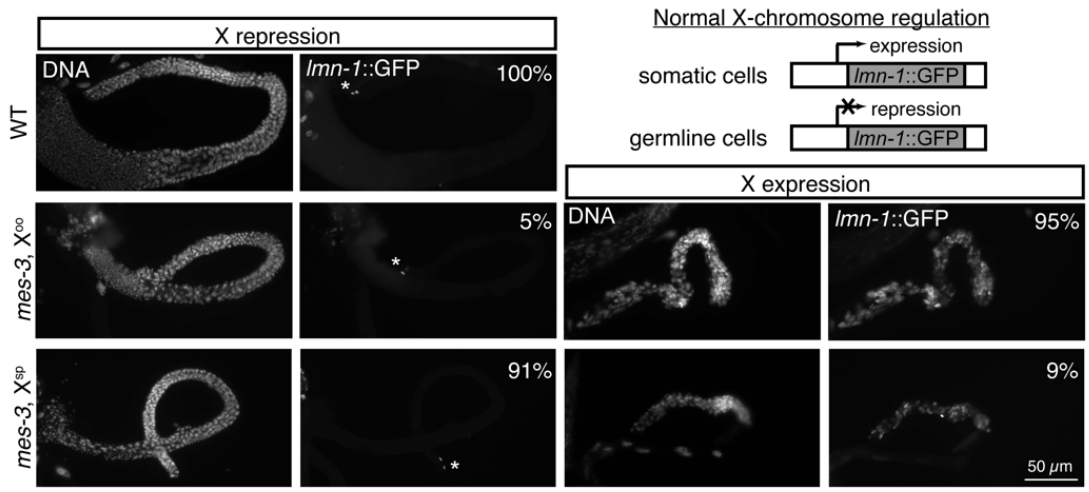

Fig. S2

X-chromosome repression in male germ lines as reported by an X-linked *lmn-1*::GFP transgene.

Repression of *lmn-1*::GFP (left) and expression (right), with percentages of germ lines showing each pattern in the top right corner, in wild-type (WT), *mes-3* XO (X^{oo}), and *mes-3* XO (X^{sp}) males. The somatic gonad distal tip cells (*) at the end of each gonad arm express the transgene. *lmn-1*::GFP expression was not observed in WT germ lines (n=77), *met-2 set-25* germ lines lacking H3K9me (n=71), or under-proliferated germ lines of *glp-4(ts)* mutants raised at the restrictive temperature (*39*) (n=81). Thus, X derepression correlates with sterility of *mes* mutants and is not a consequence simply of under-proliferation of the germ line or loss of other repressive histone marks.

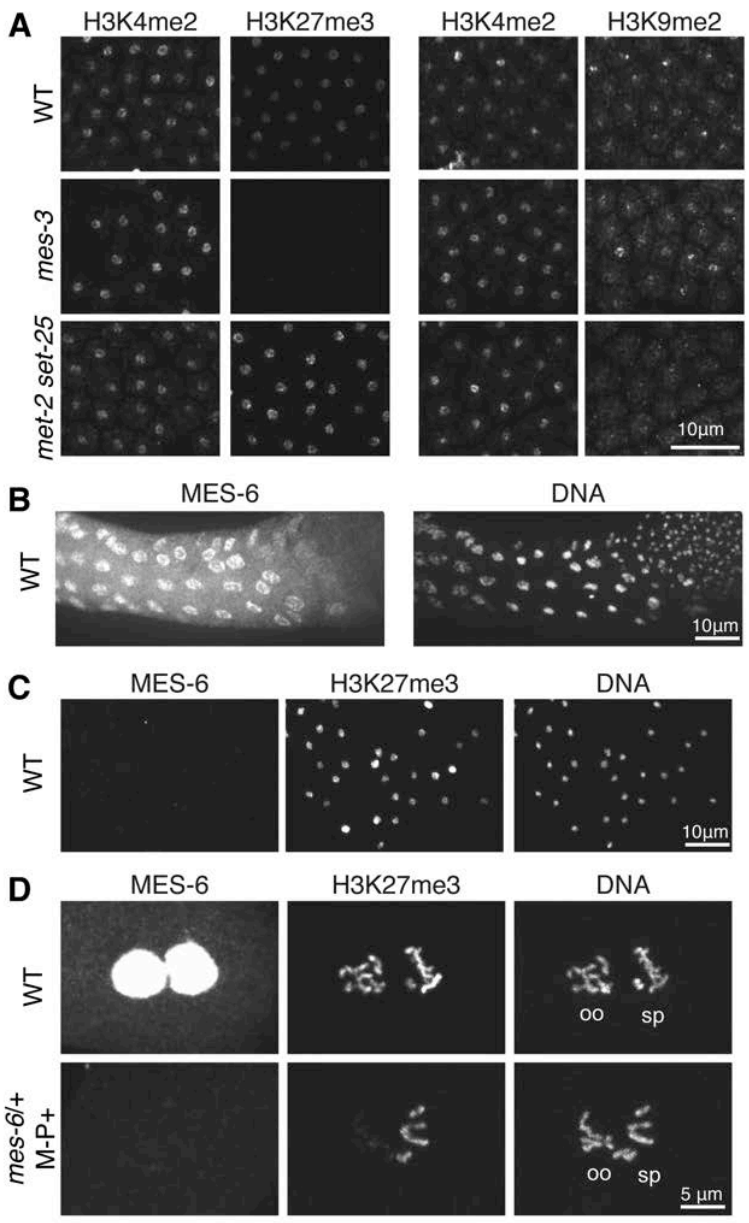

Fig. S3

Mature sperm contain H3K27me3 and H3K9me2, but not PRC2.
A) H3K27me3 and H3K9me2 are present in mature sperm in wild-type (WT) males and absent from sperm in mutant males lacking the respective HMTs, *mes-3* for H3K27me3 and *met-2 set-25* for H3K9me2. **B)** In WT male germ lines, MES-6 (a subunit of PRC2 required for HMT activity (*40*)) is concentrated in germline nuclei until sperm formation (right side of panel). **C)** MES-6 is not detectable in mature sperm; H3K27me3 is present. **D)** MES-6 is not transmitted to embryos via sperm. Images are of the oocyte (oo) and sperm (sp) pronuclei in a 1-cell WT embryo and a *mes-6/+* M-P+ 1-cell embryo. M-P+ embryos were generated by mating *mes-6* hermaphrodites with WT males, resulting in the union of *mes-6* oocytes and WT sperm. .

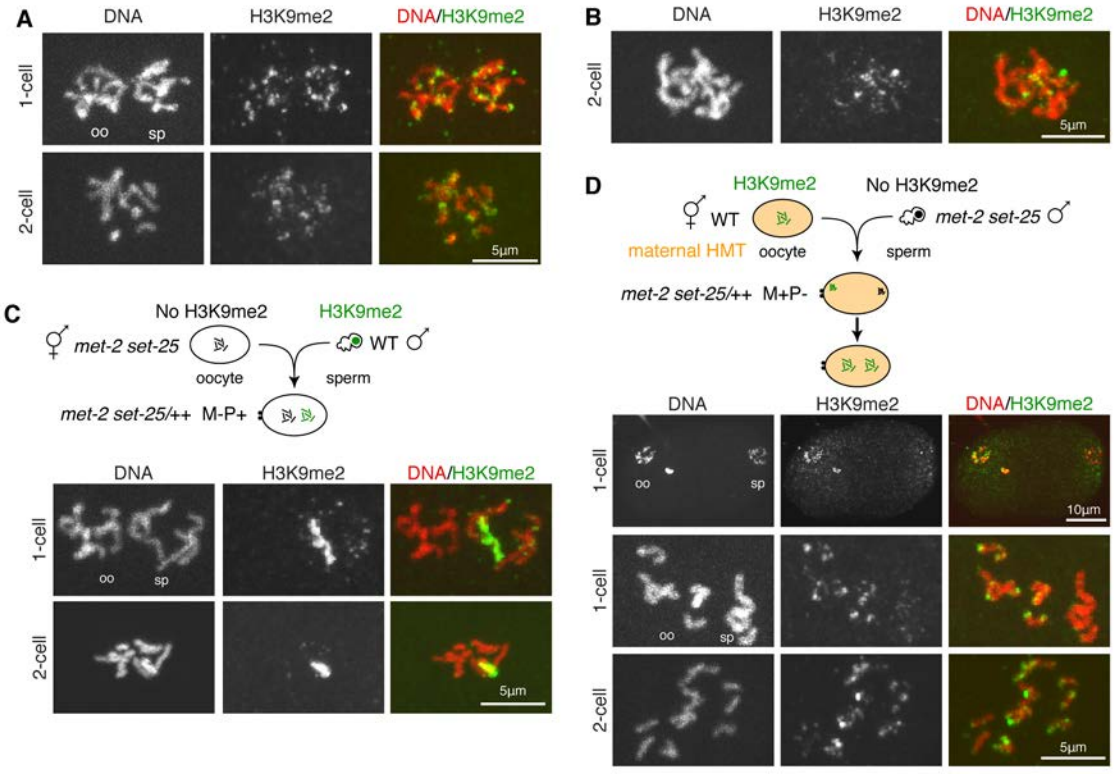

Fig. S4

H3K9me2 patterns in wild-type embryos and after inheritance from the sperm or oocyte. **A)** Images of H3K9me2 in wild-type (WT) embryos. Images are of the two pronuclei in a 1-cell embryo and a diploid nucleus in a 2-cell embryo. Embryos produced by unmated WT hermaphrodites do not show enrichment of H3K9me2 on the X. **B)** Image of H3K9me2 in one nucleus of a *mes-3* M-P- 2-cell embryo. H3K9me2 staining resembles that in WT. **C)** Diagram of oocyte and sperm union to generate embryos with H3K9me2 on the sperm chromosomes but not on the oocyte chromosomes (M-P+). Images are as for panel A. In the 1-cell, H3K9me2 is concentrated on the X inherited from male-contributed sperm, as observed in the adult male germ line (*22*). In the 2-cell, H3K9me2 inherited from the sperm persists on one chromosome, likely the X. **D)** Diagram of oocyte and sperm union to generate embryos with H3K9me2 on the oocyte chromosomes but not on the sperm chromosomes (M+P-), and with maternal HMT. Images of the two pronuclei before and after meeting in a 1-cell embryo and a diploid nucleus in a 2-cell embryo show that H3K9me2 spreads to all chromosomes. In the merge panels, DNA is in red and H3K9me2 in green. In panels A, C and D, the assignment of oocyte chromosomes (oo) and sperm chromosomes (sp) is based on the location of the polar bodies (shown in the diagrams, not in the images).

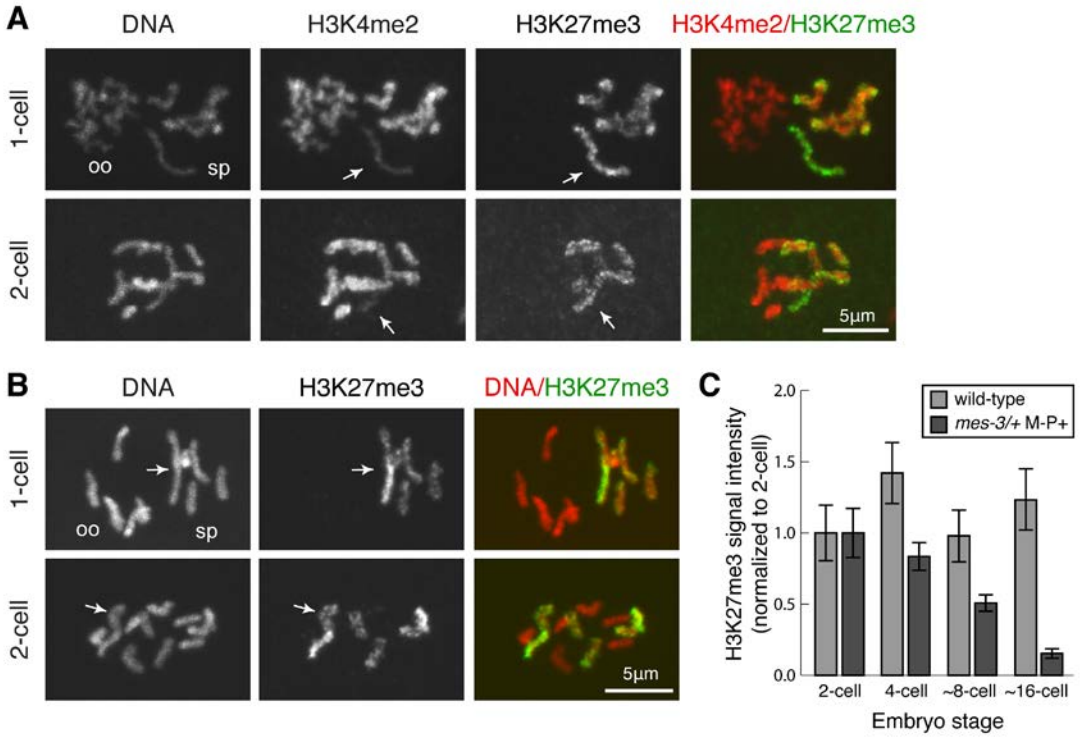

Fig. S5

In *mes-3/+* M-P+ embryos, H3K27me3 persists on two sperm-derived chromosomes and declines during successive embryonic cell divisions.

Images of embryos were generated as in Fig. 2. **A)** The sperm-derived X chromosome is more lightly stained by anti-H3K4me2 than other chromosomes (*22*). Images are of the two pronuclei in a 1-cell M-P+ embryo, and a diploid nucleus in a 2-cell M-P+ embryo, showing H3K27me3 and light H3K4me2 staining on the X chromosome from the sperm (P+) (arrow). Merge panels show H3K4me2 (red) and H3K27me3 (green). **B)** Images, as described in panel A, show H3K27me3 on a paternally derived IV-X fusion chromosome (arrow). Merge panels show DNA (red) and H3K27me3 (green). The assignment of oocyte chromosomes (oo) and sperm chromosomes (sp) in the 1-cell embryos is based on the locations of their polar bodies. **C)** The average total amount of H3K27me3 antibody staining per nucleus was determined for interphase nuclei in 2- to 16-cell embryos and normalized to the average of the 2-cell stage for each genotype (SEM, $n \geq 15$ embryos for each stage). Wild-type and *mes-3*/+ M-P+ 2-cell averages differed but were each set to 1, for comparison of later stages. Though embryos within a stage varied slightly in total number of cells, the number of cell divisions each measured cell had undergone was consistent within embryo stages; the stages analyzed represent 0, 1, 2, and 3 divisions from the 2-cell stage. In wild-type embryos, H3K27me3 level varied within a cell cycle (*11*), but did not decrease through the early embryonic cell divisions (light grey bars). In contrast, in *mes-3/+* M-P+ mutant embryos, paternally inherited H3K27me3 decreased during each early embryonic cell division (dark grey bars), as shown in Fig. 2.

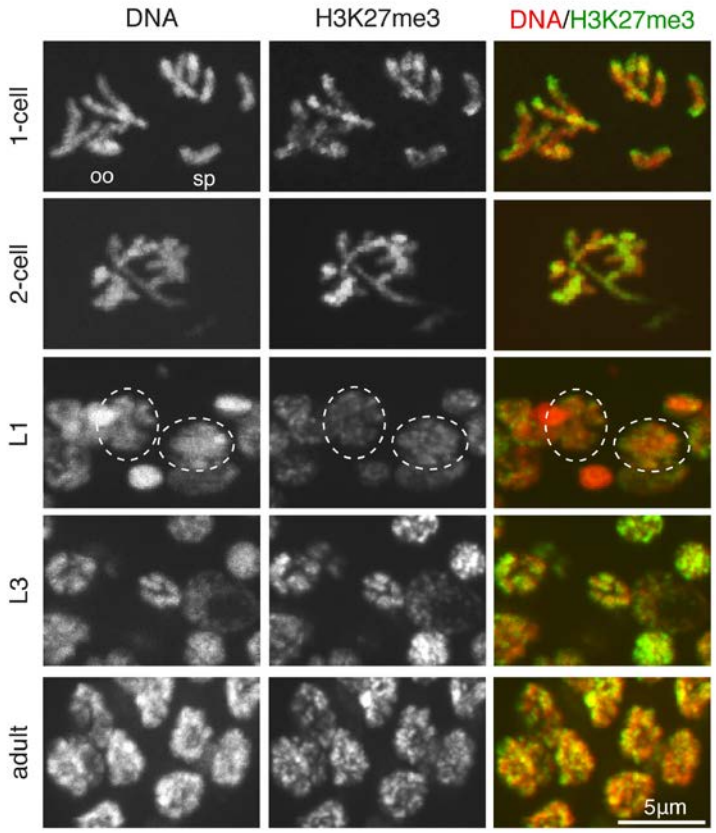

Fig. S6

Distribution of H3K27me3 in wild-type embryos and larvae, for comparison to Figs. 2-4. Images are of the two pronuclei in a 1-cell embryo and a diploid nucleus in a 2-cell embryo. Germ nuclei are circled in the L1 larva (determined by co-staining for the germ-granule marker PGL-1). Germline nuclei are shown in L3 and adult stages.

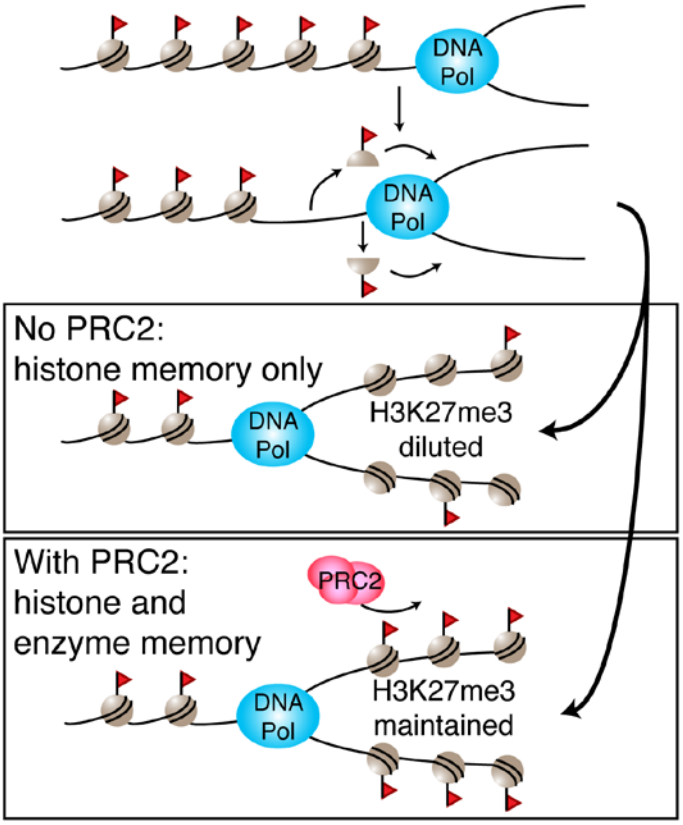

Fig. S7

Model for transmission of the memory of repression through DNA replication. Without PRC2, local passage of H3K27me3 (red flags) to daughter chromatids transmits short-term memory, for example on P+ chromosomes in M-P+ embryos (Fig. 2). With PRC2, passage of H3K27me3 and new methylation by PRC2 transmit long-term memory, for example on M+ chromosomes in M+P- embryos (Figs. 3 and 4).

References

1. R. Cao, L. Wang, H. Wang, L. Xia, H. Erdjument-Bromage, P. Tempst, R. S. Jones, Y. Zhang, Role of histone H3 lysine 27 methylation in Polycomb-group silencing. *Science* **298**, 1039–1043 (2002). Medline doi:10.1126/science.1076997

2. A. R. Pengelly, Ö. Copur, H. Jäckle, A. Herzig, J. Müller, A histone mutant reproduces the phenotype caused by loss of histone-modifying factor Polycomb. *Science* **339**, 698–699 (2013). Medline doi:10.1126/science.1231382

3. N. Iovino, F. Ciabrelli, G. Cavalli, PRC2 controls *Drosophila* oocyte cell fate by repressing cell cycle genes. *Dev. Cell* **26**, 431–439 (2013). Medline doi:10.1016/j.devcel.2013.06.021

4. K. Mochizuki, M. Tachibana, M. Saitou, Y. Tokitake, Y. Matsui, Implication of DNA demethylation and bivalent histone modification for selective gene regulation in mouse primordial germ cells. *PLOS ONE* **7**, e46036 (2012). 10.1371/journal.pone.0046036 Medline doi:10.1371/journal.pone.0046036

5. S. S. Hammoud, D. A. Nix, H. Zhang, J. Purwar, D. T. Carrell, B. R. Cairns, Distinctive chromatin in human sperm packages genes for embryo development. *Nature* **460**, 473–478 (2009). Medline

6. B. E. Bernstein, T. S. Mikkelsen, X. Xie, M. Kamal, D. J. Huebert, J. Cuff, B. Fry, A. Meissner, M. Wernig, K. Plath, R. Jaenisch, A. Wagschal, R. Feil, S. L. Schreiber, E. S. Lander, A bivalent chromatin structure marks key developmental genes in embryonic stem cells. *Cell* **125**, 315–326 (2006). Medline doi:10.1016/j.cell.2006.02.041

7. D. Pasini, A. P. Bracken, J. B. Hansen, M. Capillo, K. Helin, The Polycomb group protein Suz12 is required for embryonic stem cell differentiation. *Mol. Cell. Biol.* **27**, 3769–3779 (2007). Medline doi:10.1128/MCB.01432-06

8. E. Heard, Delving into the diversity of facultative heterochromatin: The epigenetics of the inactive X chromosome. *Curr. Opin. Genet. Dev.* **15**, 482–489 (2005). Medline doi:10.1016/j.gde.2005.08.009

9. E. E. Capowski, P. Martin, C. Garvin, S. Strome, Identification of grandchildless loci whose products are required for normal germ-line development in the nematode *Caenorhabditis elegans*. *Genetics* **129**, 1061–1072 (1991). Medline

10. L. J. Gaydos, A. Rechtsteiner, T. A. Egelhofer, C. R. Carroll, S. Strome, Antagonism between MES-4 and Polycomb repressive complex 2 promotes appropriate gene expression in *C. elegans* germ cells. *Cell Reports* **2**, 1169–1177 (2012). 10.1016/j.celrep.2012.09.019 Medline doi:10.1016/j.celrep.2012.09.019

11. C. Lanzuolo, F. Lo Sardo, A. Diamantini, V. Orlando, PcG complexes set the stage for epigenetic inheritance of gene silencing in early S phase before replication. *PLOS Genet.* **7**, e1002370 (2011). 10.1371/journal.pgen.1002370 Medline doi:10.1371/journal.pgen.1002370

12. S. Petruk, Y. Sedkov, D. M. Johnston, J. W. Hodgson, K. L. Black, S. K. Kovermann, S. Beck, E. Canaani, H. W. Brock, A. Mazo, TrxG and PcG proteins but not

methylated histones remain associated with DNA through replication. *Cell* **150**, 922–933 (2012). Medline doi:10.1016/j.cell.2012.06.046

13. L. B. Bender, R. Cao, Y. Zhang, S. Strome, The MES-2/MES-3/MES-6 complex and regulation of histone H3 methylation in *C. elegans*. *Curr. Biol.* **14**, 1639–1643 (2004). Medline doi:10.1016/j.cub.2004.08.062

14. S. Strome, W. G. Kelly, S. Ercan, J. D. Lieb, Regulation of the X chromosomes in *Caenorhabditis elegans*. *Cold Spring Harb. Perspect. Biol.* **6**, a018366 (2014). 10.1101/cshperspect.a018366 Medline doi:10.1101/cshperspect.a018366

15. C. Garvin, R. Holdeman, S. Strome, The phenotype of *mes-2*, *mes-3*, *mes-4* and *mes-6*, maternal-effect genes required for survival of the germline in *Caenorhabditis elegans*, is sensitive to chromosome dosage. *Genetics* **148**, 167–185 (1998). Medline

16. W. G. Kelly, C. E. Schaner, A. F. Dernburg, M. H. Lee, S. K. Kim, A. M. Villeneuve, V. Reinke, X-chromosome silencing in the germline of *C. elegans*. *Development* **129**, 479–492 (2002). Medline

17. J. Liu, T. Rolef Ben-Shahar, D. Riemer, M. Treinin, P. Spann, K. Weber, A. Fire, Y. Gruenbaum, Essential roles for *Caenorhabditis elegans* lamin gene in nuclear organization, cell cycle progression, and spatial organization of nuclear pore complexes. *Mol. Biol. Cell* **11**, 3937–3947 (2000). Medline doi:10.1091/mbc.11.11.3937

18. C. Beisel, R. Paro, Silencing chromatin: Comparing modes and mechanisms. *Nat. Rev. Genet.* **12**, 123–135 (2011). Medline doi:10.1038/nrg2932

19. B. D. Towbin, C. González-Aguilera, R. Sack, D. Gaidatzis, V. Kalck, P. Meister, P. Askjaer, S. M. Gasser, Step-wise methylation of histone H3K9 positions heterochromatin at the nuclear periphery. *Cell* **150**, 934–947 (2012). Medline doi:10.1016/j.cell.2012.06.051

20. D. S. Chu, H. Liu, P. Nix, T. F. Wu, E. J. Ralston, J. R. Yates 3rd, B. J. Meyer, Sperm chromatin proteomics identifies evolutionarily conserved fertility factors. *Nature* **443**, 101–105 (2006). Medline doi:10.1038/nature05050

21. J. K. Arico, D. J. Katz, J. van der Vlag, W. G. Kelly, Epigenetic patterns maintained in early *Caenorhabditis elegans* embryos can be established by gene activity in the parental germ cells. *PLOS Genet.* **7**, e1001391 (2011). 10.1371/journal.pgen.1001391 Medline doi:10.1371/journal.pgen.1001391

22. C. J. Bean, C. E. Schaner, W. G. Kelly, Meiotic pairing and imprinted X chromatin assembly in *Caenorhabditis elegans*. *Nat. Genet.* **36**, 100–105 (2004). Medline doi:10.1038/ng1283

23. R. Margueron, D. Reinberg, Chromatin structure and the inheritance of epigenetic information. *Nat. Rev. Genet.* **11**, 285–296 (2010). Medline doi:10.1038/nrg2752

24. R. Margueron, N. Justin, K. Ohno, M. L. Sharpe, J. Son, W. J. Drury 3rd, P. Voigt, S. R. Martin, W. R. Taylor, V. De Marco, V. Pirrotta, D. Reinberg, S. J. Gamblin,

Role of the polycomb protein EED in the propagation of repressive histone marks. *Nature* **461**, 762–767 (2009). Medline doi:10.1038/nature08398

25. S. Erhardt, I. H. Su, R. Schneider, S. Barton, A. J. Bannister, L. Perez-Burgos, T. Jenuwein, T. Kouzarides, A. Tarakhovsky, M. A. Surani, Consequences of the depletion of zygotic and embryonic enhancer of zeste 2 during preimplantation mouse development. *Development* **130**, 4235–4248 (2003). Medline doi:10.1242/dev.00625

26. K. Ohno, D. McCabe, B. Czermin, A. Imhof, V. Pirrotta, ESC, ESCL and their roles in Polycomb Group mechanisms. *Mech. Dev.* **125**, 527–541 (2008). Medline doi:10.1016/j.mod.2008.01.002

27. S. Kaneko, R. Bonasio, R. Saldaña-Meyer, T. Yoshida, J. Son, K. Nishino, A. Umezawa, D. Reinberg, Interactions between JARID2 and noncoding RNAs regulate PRC2 recruitment to chromatin. *Mol. Cell* **53**, 290–300 (2014). Medline doi:10.1016/j.molcel.2013.11.012

28. J. L. Rinn, M. Kertesz, J. K. Wang, S. L. Squazzo, X. Xu, S. A. Brugmann, L. H. Goodnough, J. A. Helms, P. J. Farnham, E. Segal, H. Y. Chang, Functional demarcation of active and silent chromatin domains in human HOX loci by noncoding RNAs. *Cell* **129**, 1311–1323 (2007). Medline doi:10.1016/j.cell.2007.05.022

29. F. W. Schmitges, A. B. Prusty, M. Faty, A. Stützer, G. M. Lingaraju, J. Aiwazian, R. Sack, D. Hess, L. Li, S. Zhou, R. D. Bunker, U. Wirth, T. Bouwmeester, A. Bauer, N. Ly-Hartig, K. Zhao, H. Chan, J. Gu, H. Gut, W. Fischle, J. Müller, N. H. Thomä, Histone methylation by PRC2 is inhibited by active chromatin marks. *Mol. Cell* **42**, 330–341 (2011). Medline doi:10.1016/j.molcel.2011.03.025

30. U. Brykczynska, M. Hisano, S. Erkek, L. Ramos, E. J. Oakeley, T. C. Roloff, C. Beisel, D. Schübeler, M. B. Stadler, A. H. Peters, Repressive and active histone methylation mark distinct promoters in human and mouse spermatozoa. *Nat. Struct. Mol. Biol.* **17**, 679–687 (2010). Medline doi:10.1038/nsmb.1821

31. Y. Seki, K. Hayashi, K. Itoh, M. Mizugaki, M. Saitou, Y. Matsui, Extensive and orderly reprogramming of genome-wide chromatin modifications associated with specification and early development of germ cells in mice. *Dev. Biol.* **278**, 440–458 (2005). Medline doi:10.1016/j.ydbio.2004.11.025

32. M. Saitou, M. Yamaji, Primordial germ cells in mice. *Cold Spring Harb. Perspect. Biol.* **4**, a008375 (2012). 10.1101/cshperspect.a008375 Medline

33. S. Strome, W. B. Wood, Generation of asymmetry and segregation of germ-line granules in early *C. elegans* embryos. *Cell* **35**, 15–25 (1983). Medline doi:10.1016/0092-8674(83)90203-9

34. I. Kawasaki, Y. H. Shim, J. Kirchner, J. Kaminker, W. B. Wood, S. Strome, PGL-1, a predicted RNA-binding component of germ granules, is essential for fertility in *C. elegans*. *Cell* **94**, 635–645 (1998). Medline doi:10.1016/S0092-8674(00)81605-0

35. T. A. Egelhofer, A. Minoda, S. Klugman, K. Lee, P. Kolasinska-Zwierz, A. A. Alekseyenko, M. S. Cheung, D. S. Day, S. Gadel, A. A. Gorchakov, T. Gu, P. V.

Kharchenko, S. Kuan, I. Latorre, D. Linder-Basso, Y. Luu, Q. Ngo, M. Perry, A. Rechtsteiner, N. C. Riddle, Y. B. Schwartz, G. A. Shanower, A. Vielle, J. Ahringer, S. C. Elgin, M. I. Kuroda, V. Pirrotta, B. Ren, S. Strome, P. J. Park, G. H. Karpen, R. D. Hawkins, J. D. Lieb, An assessment of histone-modification antibody quality. *Nat. Struct. Mol. Biol.* **18**, 91–93 (2011). Medline doi:10.1038/nsmb.1972

36. H. Kimura, Y. Hayashi-Takanaka, Y. Goto, N. Takizawa, N. Nozaki, The organization of histone H3 modifications as revealed by a panel of specific monoclonal antibodies. *Cell Struct. Funct.* **33**, 61–73 (2008). Medline doi:10.1247/csf.07035

37. Q. Zhou, H. Li, D. Xue, Elimination of paternal mitochondria through the lysosomal degradation pathway in *C. elegans*. *Cell Res.* **21**, 1662–1669 (2011). Medline doi:10.1038/cr.2011.182

38. J. Hodgkin, H. R. Horvitz, S. Brenner, Nondisjunction mutants of the nematode *Caenorhabditis elegans*. *Genetics* **91**, 67–94 (1979). Medline

39. M. J. Beanan, S. Strome, Characterization of a germ-line proliferation mutation in *C. elegans*. *Development* **116**, 755–766 (1992). Medline

40. C. S. Ketel, E. F. Andersen, M. L. Vargas, J. Suh, S. Strome, J. A. Simon, Subunit contributions to histone methyltransferase activities of fly and worm Polycomb group complexes. *Mol. Cell. Biol.* **25**, 6857–6868 (2005). Medline doi:10.1128/MCB.25.16.6857-6868.2005